




Cite this: *RSC Adv.*, 2022, 12, 25424

Removal of *p*-toluenesulfonic acid from wastewater using a filtration-enhanced electro-Fenton reactor†

Xueye Wang,[‡] Lehui Ren,[‡] Wengui Zha, Zhouyan Li, Ruobin Dai * and Zhiwei Wang *

Rapid global industrialization accompanies the discharge of industrial wastewater. *p*-Toluenesulfonic acid (PTSA), a kind of aromatic sulfonate that belongs to the refractory organic pollutant, is one of the most widely used chemicals in pharmaceutical, dye, petrochemical and plastic industries. In this study, we developed a filtration-enhanced electro-Fenton (FEEF) reactor to remove PTSA from synthetic wastewater. A filtration-enhanced stainless-steel mesh (FESSM) was used as the cathode. Under the optimal operating conditions of applied voltage 2.5 V, pH = 3.0, addition of 0.2 mM Fe²⁺ and 1.0 mM H₂O₂ for 120 min, the removal efficiency of PTSA (initial concentration of 100 mg L⁻¹) could reach 92.6%. Compared with the control anodic oxidation and conventional Fenton system, the FEEF system showed higher [•]OH yield and PTSA removal efficiency, with a lower effluent biological toxicity and operating cost. The enhanced mass transfer rate by the filtration in the FEEF system accelerated the regeneration of catalyst Fe²⁺ and further promoted the heterogeneous reactions. The Fe species on the surface of FESSM cathode possessed a gradient distribution, the inner layer was dominated by Fe and the outer layer was Fe³⁺. The degradation pathways of PTSA were proposed, including methyl hydroxylation, sulfonyl hydroxylation, β-hydrogen hydroxylation, and ring-opening reaction. These results demonstrate that the novel FEEF system is a promising technology for the removal of refractory organic pollutants from industrial wastewater.

Received 7th August 2022
Accepted 29th August 2022

DOI: 10.1039/d2ra04921j

rsc.li/rsc-advances

1. Introduction

Rapid global industrialization accompanies the discharge of industrial wastewater, which possibly contains a large number of refractory organic pollutants (e.g., polycyclic aromatic hydrocarbons, haloalkanes, and heterocyclic compounds).^{1,2} Refractory organic pollutants refer to the organic pollutants that are difficult to be degraded by the conventional biological wastewater treatment process.^{3,4} The accumulation of refractory organic pollutants in the discharged wastewater will severely threaten ecological environment and human health, due to their high toxicity, teratogenicity and even carcinogenicity.^{5,6}

p-Toluenesulfonic acid (PTSA), a kind of aromatic sulfonate that belongs to the refractory organic pollutant, is one of the most widely used chemicals in pharmaceutical, dye,

petrochemical and plastic industries.^{7,8} PTSA is an organic strong acid with a high corrosion ability. In addition, it has biological toxicity and non-biodegradability due to the existence of sulfonic acid functional group directly connected to the aromatic ring.⁹ Therefore, it is imperative to develop effective technologies to remove the refractory organic pollutant PTSA from wastewater.

Various technologies have been adopted to remove refractory organic pollutants from wastewater, including adsorption,¹⁰ filtration,¹¹ Fenton and ozonation.^{12–15} Among them, electro-Fenton (EF), an electrochemical advanced oxidation technology, has attracted increasing attention for the removal of refractory organic pollutants, owing to the advantages of high current efficiency and strong oxidation capacity.¹⁶ Degradation of pollutants by EF systems relies on the generated [•]OH from the reaction of (electrochemically produced) Fe²⁺ and H₂O₂.^{17–20} However, the efficiency of current EF technology is constrained by the mass transfer rates of contaminants toward the electrode, resulting in a low utilization rate of reactive oxygen species and thereby an inadequate removal rate of contaminants. For instance, Özcan *et al.* investigated naphthol blue black (NBB) removal by EF, and found that the complete decolorization of NBB took 180 min.¹³ Santana-Martínez *et al.* found that under the condition of pH = 3 and current density 40

State Key Laboratory of Pollution Control and Resource Reuse, Advanced Membrane Technology Center of Tongji University, Shanghai Institute of Pollution Control and Ecological Security, School of Environmental Science and Engineering, Tongji University, Shanghai 200092, PR China. E-mail: dairuobin@tongji.edu.cn; zwwang@tongji.edu.cn

† Electronic supplementary information (ESI) available. See <https://doi.org/10.1039/d2ra04921j>

‡ These authors contributed equally to the work.



mA cm^{-2} , the TOC removal of 4-chlorophenol with initial concentration of 100 mg L^{-1} by EF was only 45% after 120 min.¹⁸ Although some novel electrodes have been developed, such as gas diffusion electrode,²¹ three-dimensional electrode,²² and carbon nanotube modified electrode,²³ the drawback of the limited mass transfer rate was still not well addressed. Meanwhile, the capital expenditures of these electrodes are quite high and the scale-up of these electrodes in real wastewater treatment is still challenging. We hypothesize that an EF system based on a filtration-enhanced stainless-steel mesh (FESSM) cathode can be a cost-effective method to achieve favorable removal of PTSA. The filtration-enhanced system may have several advantages: (i) convective mass transfer toward the filtration-enhanced cathode surface could strengthen the contact oxidation of PTSA by $\cdot\text{OH}$; (ii) concentration polarization of Fe species on the cathode surface could accelerate the heterogeneous Fenton reaction; (iii) solid-liquid separation and EF reaction could be achieved simultaneously.

Herein, we developed a filtration-enhanced electro-Fenton (FEEF) reactor, with SSM filtration module as the cathode and graphite plate as the anode, to achieve efficient removal of the PTSA. The PTSA removal performance and influencing factors of FEEF system were investigated. The PTSA removal and the production of $\cdot\text{OH}$ of the FEEF system were compared with conventional Fenton and anodic oxidation systems. The Fe-mediated mechanism of PTSA oxidation was clarified. The degradation pathway of PTSA was proposed after identifying the intermediate products. Moreover, the effluent biotoxicity and energy consumption of the FEEF reactor for PTSA degradation was evaluated.

2. Materials and methods

2.1. Materials

All reagents and chemicals were analytical grade unless stated otherwise. HPLC-grade methanol (CH_3OH) was supplied by Sigma-Aldrich (USA). Hydrogen peroxide (H_2O_2), phosphoric acid, and ferrous sulfate heptahydrate were purchased from Sinopharm (China). PTSA was provided by Rhawn (China). All solutions were prepared by deionized water ($18.2 \text{ M}\Omega \text{ cm}$), and the pH of solutions was adjusted by $0.1 \text{ M H}_2\text{SO}_4$ or 0.1 M NaOH . Unless otherwise specified, the pH value of the solution at the concentration of PTSA was 3.

2.2. FEEF setup and operation

The electrochemical degradation of PTSA was carried out in a 300 mL FEEF reactor (Fig. 1) in a constant voltage mode, using two graphite plates as the anode and a stainless-steel mesh (SSM) filtration module as the cathode. The graphite plates were placed parallelly on both sides of the SSM filtration module with a spacing of 1 cm. The SSM filtration module (with dimension = $5 \text{ cm} \times 8 \text{ cm}$, thickness = 1 cm, the total effective filtration area 36 cm^2) was assembled by binding two SSMs (pore size = $48 \mu\text{m}$) to two sides of a polyvinyl chloride (PVC) bracket. The SSM filtration module acted as both the cathode and the filter.²⁴ DC power was connected with the cathode and the anode of the FEEF system through the wire. According to the linear sweep voltammetry (LSV) curve (Fig. S1†), the voltage of 0–3.0 V was selected for the experiment. An air diffuser was installed at the bottom of the reactor for aeration with a flow rate 400 mL min^{-1} .

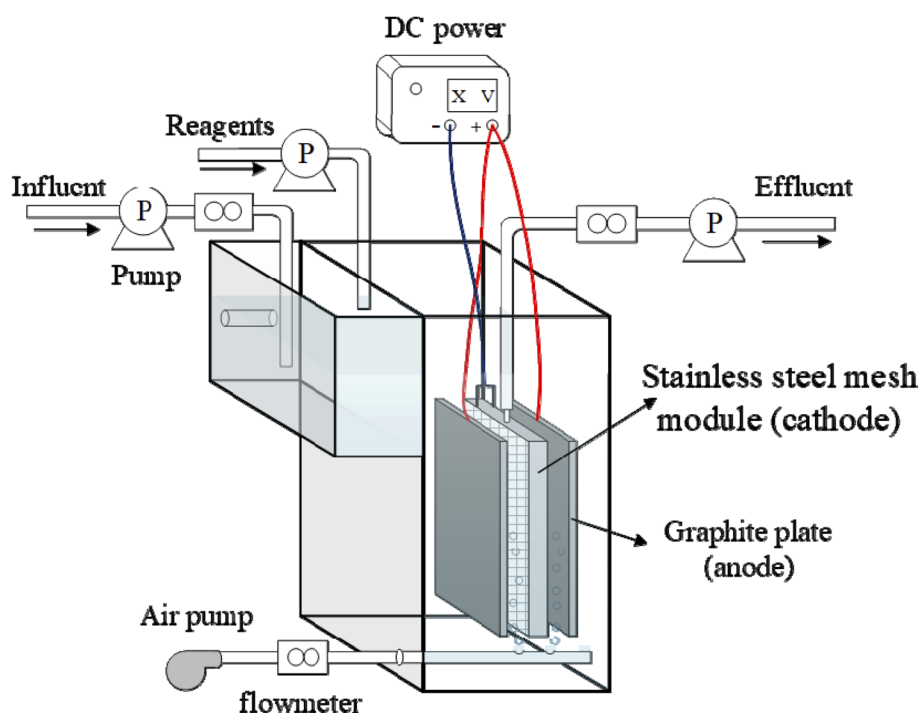


Fig. 1 Schematic of filtration-enhanced electro-Fenton (FEEF) experimental setup.

All experiments of FEEF reactor operation were conducted in an internally circulated flow-through mode. In this mode, the synthetic PTSA-contained wastewater was filtrated through the SSM filtration module (with a flux of $333.3 \text{ L m}^{-2} \text{ h}^{-1}$) and returned to the reactor, where the electrolysis time equaled to the sampling time. Compared with the traditional immersed plate electrode and flow-by mode, the flow-through mode can reduce the boundary layer and enhance the convective mass transfer of pollutants from the bulk solution to the cathode surface.^{25,26} Samples collected from the reactor were filtered *via* $0.45 \mu\text{m}$ polyether sulfone filter before further measurement. Reagents (*i.e.*, H_2O_2 or FeSO_4) were added (if needed) by syringes prior to the electrolysis. To further investigate the efficiency of FEEF system, the two systems were compared, *i.e.*, the traditional Fenton system without applied voltage and the anodic oxidation system without Fe^{2+} and H_2O_2 . In addition, "Fenton + AO" refers to the similar one (or the control) to FEEF system without the filtration capacity.

2.3. Analytical methods

The concentration of PTSA was analyzed using a reversed-phase high performance liquid chromatography (HPLC, Agilent 1290, USA).⁸ The degradation intermediates of PTSA were first purified using solid-phase extraction (SPE) column to remove salinity and then determined by a liquid chromatograph mass spectrometer (LC-MS) (Waters, Thermo, Q-Exactive) equipped with ACQUITY UPLC HSS T3 column (detailed in Text S1†). The iron species in the solution, including aqueous Fe(II) , Fe(III) , and colloidal Fe(III) (oxyhydro) oxide, were quantified according to the phenanthroline spectrometric method.⁸ The concentration of H_2O_2 was analyzed using a UV-vis spectrophotometer (PERSEE, Beijing, China) according to the metavanadate method.²⁷ Solution pH was determined by a pH meter (HQ40d, Hach, USA). The toxicity of samples using *Vibrio fischeri* (NRRL B-11177) was measured according to a standard method (ISO 11348-3).

2.4. Analysis of energy cost

The operating cost of the FEEF system included the electrical consumption of DC power supply and aeration pump, the cost of possible addition of chemicals, and the cost of sludge disposal. The specific calculation formula and parameters of the operating costs are shown in Table 1.

Table 1 Calculation formulas and key parameters of treatment cost

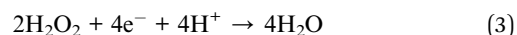
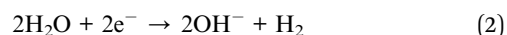
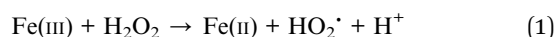
Items	Cost per unit	key parameters
DC power supply	0.11 \$ per kW h	$Q = \frac{E \times I \times \text{HRT}_a}{1000V}$ 1.2 kW ($\text{m}^3 \text{ gas min}^{-1}$) ⁻¹
Aeration	0.11 \$ per kW h	
$\text{FeSO}_4 \cdot 7\text{H}_2\text{O}$ (98%)	74.9 \$ per t	60% moisture content
H_2O_2 (27.5%)	224.7 \$ per t	
Iron sludge disposal	74.9 \$ per t	

^a Q is the electrolytic energy consumption (kW h m^{-3}), E is the applied voltage (V), I is the mean current (A), HRT is hydraulic retention time (electrolytic time) (h), V is the reactor volume (m^3).

3. Results and discussion

3.1. Electrochemical degradation of PTSA by FEEF reactor

3.1.1. Effect of applied voltage. Fig. 2a shows the PTSA degradation performance of the FEEF system at different applied different voltages (0–3.0 V). Note that additional Fe^{2+} and H_2O_2 were added into the system to ensure the PTSA removal efficiency at the optimized condition. Under the same condition ($[\text{PTSA}]_0 = 100 \text{ mg L}^{-1}$, 0.2 mM Fe^{2+} and $1.0 \text{ mM H}_2\text{O}_2$), the removal efficiency of PTSA by the FEEF system with applied voltage was higher than that without applied voltage, because the electrochemical reduction reaction on the cathode surface could accelerate the regeneration of Fe(II) and promote the formation of $\cdot\text{OH}$. However, the reaction of Fe(III) and H_2O_2 to generate Fe(II) was regarded as the rate-limiting step of conventional Fenton reaction, and H_2O_2 would be consumed in this process (eqn (1)).²⁸ Moreover, the PTSA removal by FEEF system is closely associated with applied voltage. The removal efficiency was increased from 78.5% to 98.0% as the applied voltage increased from 2.0 V to 3.0 V. When the applied voltage was higher than 2.5 V, the removal efficiency of PTSA was only slightly improved. The reason might be that increasing voltage within a certain range could contribute to promote the regeneration of Fe(II) and further accelerated the production of more $\cdot\text{OH}$ (Fig. S2†). However, when the applied voltage exceeded 3.0 V, the side reaction (eqn (2) and (3)) was intensified and accompanied the consumption of H_2O_2 .²⁹



3.1.2. Effect of pH. Fig. 2b shows the effect of different pH (pH = 2.5, 3.0, 3.5, and 4.0) on the PTSA removal efficiency in the FEEF system. The highest removal efficiency of PTSA was observed at pH = 3.0, which was close to the results reported in previous literature that the optimal pH of conventional Fenton reaction was 2.8.^{30,31} Moreover, when the pH value was higher than 3.0, the removal efficiency of PTSA decreased rapidly. The reason was that the higher pH inhibited the regeneration of Fe(II) through the cathodic reduction of Fe(III) .^{32,33} When the pH was 2.5, the removal efficiency of PTSA in FEEF system decreased slightly due to the influence of hydrogen evolution reaction (eqn (2)).³⁴ These results showed that pH = 3 was the optimal pH value for the PTSA removal by the FEEF system.

3.1.3. Effect of initial concentration of PTSA. To evaluate the effect of the initial PTSA concentration on the removal efficiency of FEEF system (or the PTSA treatment capacity of the FEEF system), the experiments were conducted under PTSA concentrations of 50, 100, 150, and 200 mg L^{-1} . As shown in Fig. 2c, the removal efficiency of PTSA decreased with the increase of PTSA initial concentration. For example, when the initial concentration of PTSA increased from 50 mg L^{-1} to 200 mg L^{-1} , the removal efficiency of PTSA decreased from



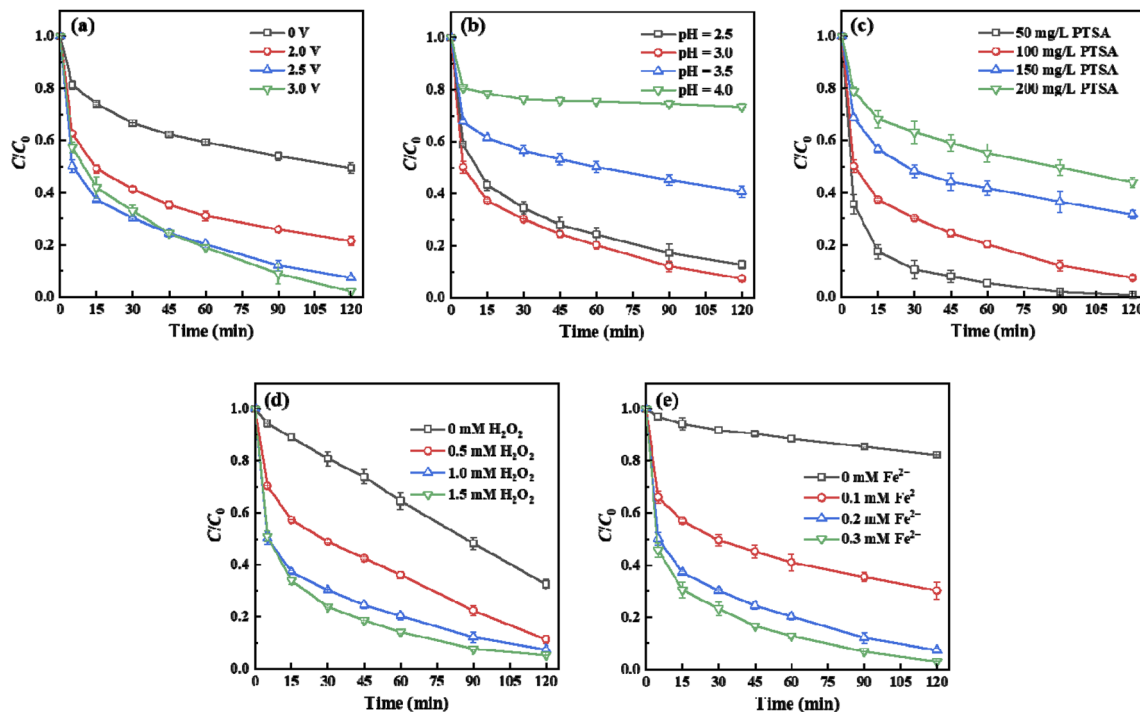


Fig. 2 The effects of (a) applied voltage, (b) solution pH, (c) initial PTSA concentration, (d) H_2O_2 concentration, and (e) Fe^{2+} concentration on the removal of PTSA by the FEEF system. Experimental conditions: (a) $[\text{PTSA}]_0 = 100 \text{ mg L}^{-1}$, pH = 3.0, 0.2 mM Fe^{2+} and 1.0 mM H_2O_2 dosage. (b) $[\text{PTSA}]_0 = 100 \text{ mg L}^{-1}$, applied voltage = 2.5 V, 0.2 mM Fe^{2+} and 1.0 mM H_2O_2 dosage. (c) Applied voltage = 2.5 V, pH = 3.0, 0.2 mM Fe^{2+} and 1.0 mM H_2O_2 dosage. (d) $[\text{PTSA}]_0 = 100 \text{ mg L}^{-1}$, applied voltage = 2.5 V, pH = 3.0, 0.2 mM Fe^{2+} dosage. (e) $[\text{PTSA}]_0 = 100 \text{ mg L}^{-1}$, applied voltage = 2.5 V, pH = 3.0, 1.0 mM H_2O_2 dosage.

99.3% to 56.1% after 120 min electrolysis under the condition of 2.5 V applied voltage, 0.2 mM Fe^{2+} and 1.0 mM H_2O_2 . This is because the PTSA oxidation was constrained by the amount of generated $\cdot\text{OH}$. When the initial concentration of PTSA was low, the generated $\cdot\text{OH}$ could react with more proportion of PTSA, resulting in higher removal efficiency of PTSA.

3.1.4. Effect of H_2O_2 concentration. The effect of different H_2O_2 dosage on the removal efficiency of PTSA in the FEEF system was further investigated. As shown in Fig. 2d, the FEEF system without adding H_2O_2 still exhibited stable PTSA removal (67.6% after electrolysis 120 min), which might be attributed to the generation of H_2O_2 on the FESSM cathode surface by two-electron electrochemical reduction.³⁵ As expected, the addition of H_2O_2 would accelerate the degradation of PTSA. For example, under the condition of 1.0 mM H_2O_2 , only a quarter of the time was needed to achieve the same PTSA removal efficiency (67.6%) under the condition of 0 mM H_2O_2 . The reason was that the addition of H_2O_2 , as one of the key Fenton reagents, could promote the homogeneous Fenton reaction.³⁶ Meanwhile, the heterogeneous Fenton reaction occurring on the FESSM cathode surface was enhanced by adding H_2O_2 . It should be noted that when the dosage of H_2O_2 exceeded 1.0 mM, the removal efficiency of PTSA was not significantly improved, which might be attributed to the negative effects of excessive H_2O_2 , such as the scavenging effect on $\cdot\text{OH}$ and the accelerated electrocatalytic decomposition of H_2O_2 , thereby reducing the utilization efficiency of oxidants.³⁷

3.1.5. Effect of Fe^{2+} concentration. The effect of different Fe^{2+} dosage on the removal efficiency of PTSA by the FEEF system was further investigated. As shown in Fig. 2e, the removal efficiency of PTSA substantially increased after adding Fe^{2+} . For example, when Fe^{2+} dosage increased from 0 mM to 0.2 mM, the removal efficiency of PTSA (electrolysis for 120 min) increased from 17.7% to 92.6%. The reason might be that the occurrence of homogeneous Fenton reaction and the increase of Fe^{2+} loading on the FESSM cathode surface (enhanced the heterogeneous Fenton reaction).³⁸ However, when the Fe^{2+} concentration was higher than 0.2 mM, the removal efficiency of PTSA was not significantly improved, which might be due to the excessive Fe^{2+} reaction with $\cdot\text{OH}$.³⁹

3.2. Enhanced oxidation of PTSA in FEEF system

As shown in Fig. 3a, the removal efficiency of PTSA in the FEEF system was found higher than that in conventional Fenton or anodic oxidation (AO) system. Interestingly, the removal efficiency of PTSA was even much greater than the mathematical addition of the removal efficiency of the Fenton and AO systems ("Fenton + AO"). $\cdot\text{OH}$ production was further evaluated by adding excessive isopropanol (100 mM) as a probe compound.^{24,40} It can be seen from Fig. 3b that the $\cdot\text{OH}$ production (represented by acetone, the oxidized product of isopropanol) in the FEEF system within 60 min was much larger than that of anodic oxidation and Fenton systems, indicating that the FEEF system enhanced the $\cdot\text{OH}$ production in the



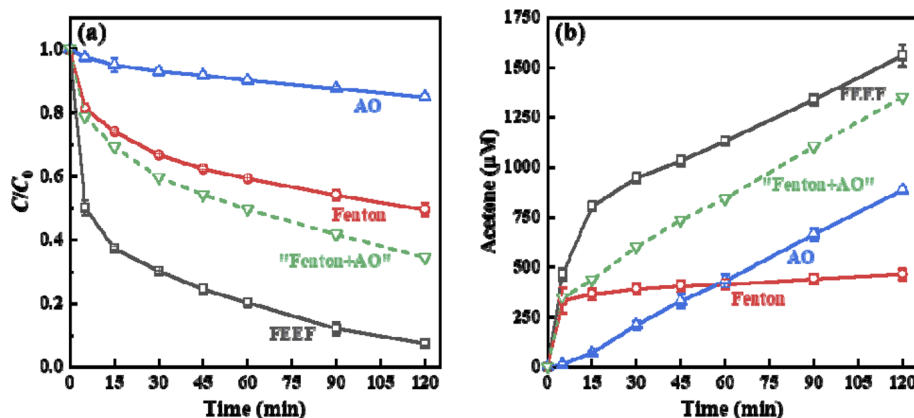


Fig. 3 (a) The removal performance of PTSA, and (b) the $\cdot\text{OH}$ production under different systems. Experimental condition of FEEF: $[\text{PTSA}]_0 = 100 \text{ mg L}^{-1}$, voltage = 2.5 V, pH 3.0, 0.2 mM Fe^{2+} and $1.0 \text{ mM H}_2\text{O}_2$ dosage. Experimental condition of anodic oxidation: $[\text{PTSA}]_0 = 100 \text{ mg L}^{-1}$, voltage = 2.5 V, pH 3.0. Experimental condition of Fenton: $[\text{PTSA}]_0 = 100 \text{ mg L}^{-1}$, pH 3.0, 0.2 mM Fe^{2+} and $1.0 \text{ mM H}_2\text{O}_2$ dosage.

system. The reason was: (i) Fe(II) could capture H_2O_2 (from cathode generation or external addition) at the FESSM cathode interface or in bulk solution, thereby improving the utilization efficiency of oxidants;²⁶ (ii) the applied voltage could accelerate the regeneration of Fe(II) , thereby promoting the heterogeneous Fenton reaction at the cathode interface.³⁸ These results indicated that the FEEF system has better potential for the treatment of refractory organic compounds.

3.3. Proposed Fe-mediated mechanisms of PTSA oxidation

The regeneration process of Fe(II) is one of the key rate-limiting steps of Fenton reaction. To clarify the Fe-mediated mechanisms of PTSA oxidation in FEEF system, the distribution and concentration changes of Fe (e.g. Fe^0 , Fe(II) , Fe(III) , and colloidal Fe) in the homogeneous solution and the FESSM cathode surface were investigated. Fig. 4a shows the distribution of Fe species in the homogeneous solution of the FEEF system. Fe^{2+} was rapidly converted to Fe^{3+} by homogeneous Fenton reaction within 0–5 min, and accompanied by the consumption of H_2O_2 (Fig. S2†). With the increasing consumption of H_2O_2 , the Fenton reaction rate decreased, resulting in the consumption rate of Fe^{2+} slower than the electrochemical regeneration rate. Furthermore, the Fe species gradually transformed from Fe^{3+} to Fe^{2+} , and resulting in the existence of majority of Fe species in aqueous solution in the form of Fe^{2+} after 30 min.

The elemental chemical states of Fe on the surface of FESSM cathode in the FEEF system was further analyzed by XPS and compared with the original SSM. As shown in Fig. 4b–d, the surface of the original SSM was mainly composed of Fe(II) and Fe(III) . After electrochemical experiment, the proportion of Fe(III) on the FESSM cathode surface increased greatly and existed in the form of FeOOH , and the Fe species in bulk solution was mainly Fe(II) . These results indicated that Fe(III) on the FESSM cathode surface was derived from the oxidation of Fe(II) by heterogeneous Fenton reaction rather than the adsorption of Fe species in bulk solution. Moreover, it was found that the FESSM cathode was mainly composed of elemental Fe with a small amount of Fe(II) and Fe(III) after cleaning the Fe sludge on the cathode surface. This result

suggested that the gradient distribution of Fe species (Fe-Fe(III) from inside to outside) appeared on the FESSM cathode in the electrochemical reaction process, which accelerated the electron transfer in heterogeneous Fenton reaction.²³

Based on the above results and previous studies, the PTSA degradation mechanism in the FEEF system is illustrated in Fig. 5. The FESSM cathode could produce H_2O_2 through oxygen reduction.⁴¹ Subsequently, the FESSM cathode increased the convective mass transfer of the PTSA, iron species and H_2O_2 toward the cathode, ensuring the electron transfer rate of iron species to the FESSM cathode surface and accelerating the heterogeneous Fenton reaction to produce more $\cdot\text{OH}$. Consequently, the oxidation of PTSA was enhanced in the FEEF system.³²

3.4. The degradation pathways of PTSA

To further unravel the degradation pathway of PTSA in FEEF system, the degradation intermediates of PTSA at 120 min were determined by LC-MS (Q-Exactive). Based on the identified intermediate products (Fig. S3–S5†), the electrochemical oxidation degradation pathway of PTSA was proposed (Fig. 6).

In FEEF system, the oxidant produced by the electrochemical oxidation process attacked PTSA from three reaction sites. Firstly, hydrogen atom on methyl group was attacked by $\cdot\text{OH}$, resulting in the conversion of methyl group to $-\text{CH}_2\text{OH}$, $-\text{CHO}$ and $-\text{COOH}$ (i.e., 4-sulfobenzyl alcohol (EP1), 4-sulfobenzaldehyde (EP2), and 4-sulfobenzoate (EP3)), and then the $-\text{COOH}$ was further replaced by $-\text{OH}$ to achieve methyl hydroxylation.⁸ The second pathway was the cleavage of C–S bond by $\cdot\text{OH}$ attack, and the sulfonyl group was replaced by $-\text{OH}$ to form intermediate *p*-methylphenol (EP5).³² Furthermore, these aromatic compounds such as *p*-methylphenol (EP5) and 4-hydroxybenzenesulfonic acid (EP4) could be further oxidized to hydroquinone (EP11) and benzoquinone (EP12, yellow) through the successive oxidation of $\cdot\text{OH}$.⁴² The observed phenomenon that the color of the solution gradually changed from transparent to light yellow also supports this pathway. In addition, according to the literature, the third pathway is that β -hydrogen of benzene and sulfonic group were attacked by $\cdot\text{OH}$ to form



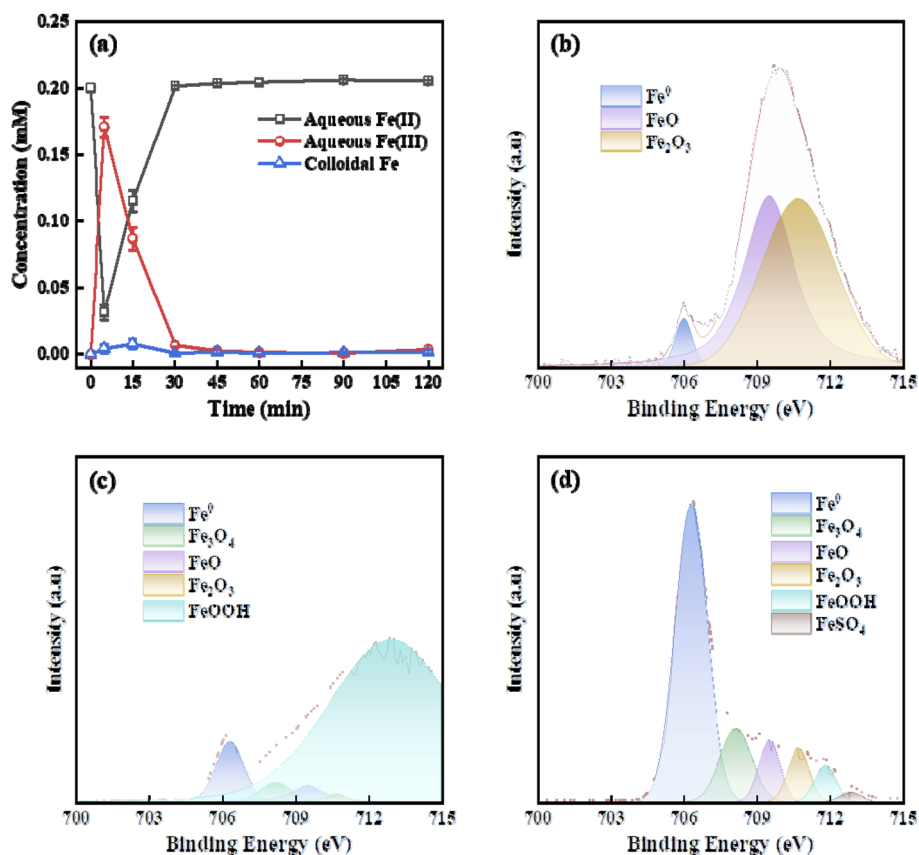


Fig. 4 (a) Changes of Fe species in homogeneous solution of FEEF system, XPS spectra of Fe species on (b) pristine steel mesh, (c) FESSM cathode after electrochemical experiment, (d) FESSM cathode after electrochemical experiment and cleaning the Fe sludge adsorbed on cathode surface. Experimental conditions: [PTSA]₀ = 100 mg L⁻¹, applied voltage = 2.5 V, pH = 3.0, 0.2 mM Fe²⁺ and 1.0 mM H₂O₂ dosage.

substances such as 2, 4, 6-trihydroxybenzoic acid (EP9).^{13,43} When [•]OH is sufficient, hydroquinone (EP12) and 2, 4, 6-trihydroxybenzoic acid (EP9) would further undertake the ring-opening reactions of the benzene to form carboxylic acids,

and finally mineralized to CO₂ and H₂O.⁸ In addition, the change of chemical oxygen demand (COD) concentration was measured to evaluate the mineralization of PTSA in FEEF system. It was found that the removal efficiency of COD was

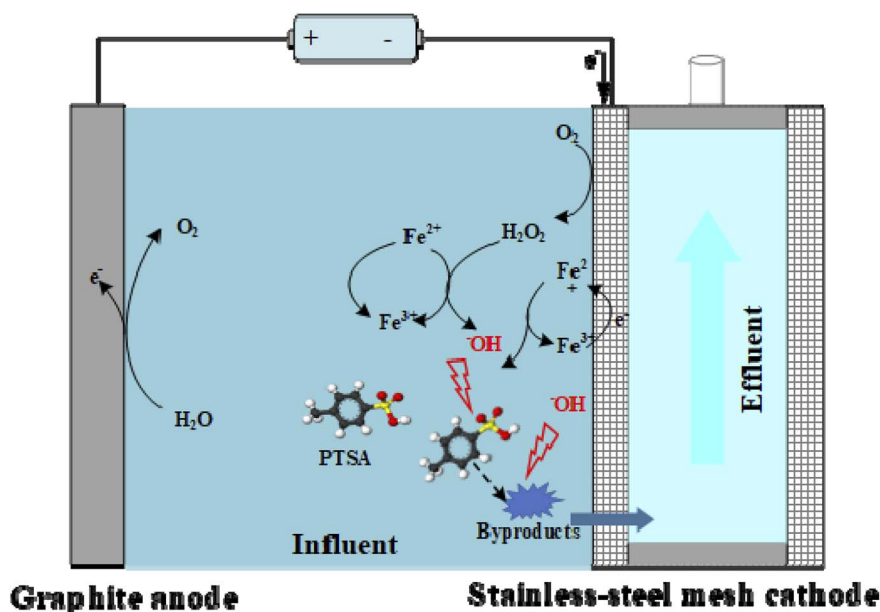


Fig. 5 Schematic of the Fe-mediated PTSA degradation mechanism in the FEEF system.

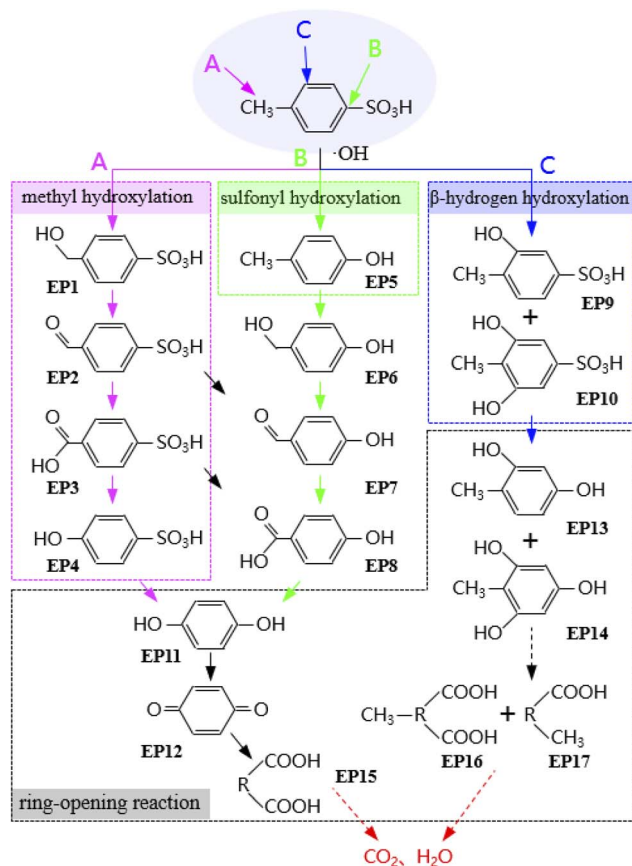


Fig. 6 The degradation pathways of PTSA in FEEF system.

35.5% after 120 min electrolysis (Fig. S6†), indicating that the system had a certain mineralization ability.

3.5. Analysis of effluent toxicity

To investigate the environmental risk of the treated PTSA-containing wastewater by the FEEF system, the biotoxicity of the influent and effluent samples of FEEF was tested by *Vibrio fischeri* at the initial PTSA concentration of 100 mg L^{-1} , and compared with the conventional Fenton system. As shown in Fig. 7, the effluent biotoxicity of FEEF system decreased with the increase of electrolysis time. For example, the inhibition of luminescence was 4.9% after 60 min of electrolysis, which was much lower than that of the influent (29.1%). This phenomenon indicated that the FEEF system significantly reduced the biological toxicity of PTSA-containing wastewater. Moreover, it is worth noting that the effluent toxicity of the conventional Fenton system was higher than that of the influent, indicating that some intermediates with higher microbial toxicity might be produced. The above results showed that FEEF system was more effective in toxicity removal compared to Fenton system.^{43,44}

3.6. Energy consumption

Operating cost is an important parameter to evaluate the economic feasibility of FEEF system in treating refractory industrial wastewater. In this work, we not only consider the

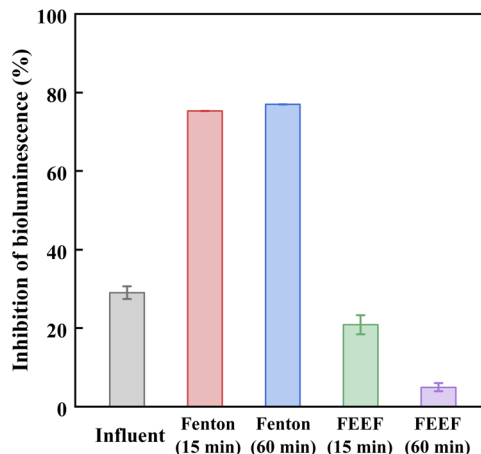


Fig. 7 Influent and effluent biotoxicity in FEEF system and Fenton system.

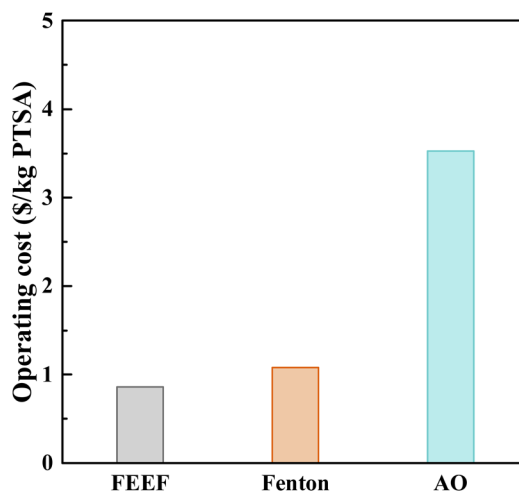


Fig. 8 Operating cost of FEEF, anodic oxidation, and Fenton system.

power consumption, but also consider the reagent cost and iron sludge treatment cost (Table S1†). As shown in Fig. 8, under the operating conditions of applied voltage 2.5 V, pH 3.0, addition of 0.2 mM Fe^{2+} and $1.0 \text{ mM H}_2\text{O}_2$, the operation cost of FEEF system was 0.86 \$ per kg PTSA, which was only 80% of conventional Fenton system or 24% of anodic oxidation system. The FEEF system improved the removal efficiency of PTSA and reduced energy consumption by filtration-enhanced electro-Fenton. In addition, compared with the other Fenton systems, the FEEF system has higher PTSA removal efficiency (Table S2†). Overall, the FEEF system has a great potential to treat refractory industrial wastewater with high efficiency and operation cost. Our study provides a new technical solution for the treatment of actual refractory industrial wastewater.

4. Conclusions

In this study, a novel and cost-effective FEEF reactor with filtration-enhanced cathode was developed to remove PTSA.



Under the optimal operating conditions of applied voltage 2.5 V, pH = 3.0, addition of 0.2 mM Fe²⁺ and 1.0 mM H₂O₂ for 120 min, the removal efficiency of PTSA (initial concentration of 100 mg L⁻¹) reached 92.6%. Compared with anodic oxidation, conventional Fenton system and reported photo-Fenton system, the FEEF system showed higher [•]OH yield and PTSA removal efficiency, with a lower effluent biological toxicity and operating cost. The enhanced mass transfer rate by the filtration in the FEEF system accelerated the regeneration of catalyst Fe²⁺ and further promoted the heterogeneous reactions. The Fe species on the surface of FESSM cathode possessed a gradient distribution, the inner layer was dominated by Fe and the outer layer was Fe(III). The degradation pathways of PTSA were proposed, including methyl hydroxylation, sulfonyl hydroxylation, β -hydrogen hydroxylation, and ring-opening reaction. These results demonstrate that the novel FEEF system is a promising technology for the removal of refractory organic pollutants from industrial wastewater. However, the stability and feasibility of FEEF system in actual wastewater containing refractory organic pollutants needs to be further investigated in the future.

Author contributions

Xueye Wang: conceptualization, investigation, supervision. Lehui Ren: investigation, writing-original draft preparation. Wengui Zha: investigation, data curation, writing-original draft preparation. Zhouyan Li: investigation. Ruobin Dai: supervision, writing—review and editing. Zhiwei Wang: conceptualization, writing—review and editing, funding acquisition.

Conflicts of interest

The authors declare no competing interests.

Acknowledgements

We thank the National Key Research and Development Program of China (Grant 2019YFC0408200), the National Natural Science Foundation of China (Grant 51838009), and the Shanghai Sailing Program (Grant 22YF1450700) for the financial support of the work.

References

- H. Luo, Y. Zeng, D. He and X. Pan, Application of iron-based materials in heterogeneous advanced oxidation processes for wastewater treatment: A review, *Chem. Eng. J.*, 2021, **407**, 127191.
- J. Zou, J. Ma, L. Chen, X. Li, Y. Guan, P. Xie and C. Pan, Rapid Acceleration of Ferrous Iron/Peroxymonosulfate Oxidation of Organic Pollutants by Promoting Fe(III)/Fe(II) Cycle with Hydroxylamine, *Environ. Sci. Technol.*, 2013, **47**, 11685–11691.
- F. Ghanbari and M. Moradi, Application of peroxymonosulfate and its activation methods for degradation of environmental organic pollutants: Review, *Chem. Eng. J.*, 2017, **310**, 41–62.
- Q. Yang, Y. Ma, F. Chen, F. Yao, J. Sun, S. Wang, K. Yi, L. Hou, X. Li and D. Wang, Recent advances in photo-activated sulfate radical-advanced oxidation process (SR-AOP) for refractory organic pollutants removal in water, *Chem. Eng. J.*, 2019, **378**, 122149.
- C. Zhao, J. Xu, D. Shang, Y. Zhang, J. Zhang, H. Xie, Q. Kong and Q. Wang, Application of constructed wetlands in the PAH remediation of surface water: A review, *Sci. Total Environ.*, 2021, **780**, 146605.
- T. O. Ajiboye, O. A. Oyewo and D. C. Onwudiwe, Simultaneous removal of organics and heavy metals from industrial wastewater: A review, *Chemosphere*, 2021, **262**, 128379.
- B. Stöffler and G. Luft, Oxidative degradation of p-toluenesulfonic acid using hydrogen peroxide, *Chemosphere*, 1999, **38**, 1035–1047.
- J. Zheng, J. Ma, Z. Wang, S. Xu, T. D. Waite and Z. Wu, Contaminant removal from source waters using cathodic electrochemical membrane filtration: Mechanisms and Implications, *Environ. Sci. Technol.*, 2017, **51**, 2757–2765.
- S. P. Kamble, S. B. Sawant and V. G. Pangarkar, Heterogeneous photocatalytic degradation of p-toluenesulfonic acid using concentrated solar radiation in slurry photoreactor, *J. Hazard. Mater.*, 2007, **140**, 149–154.
- A. M. Amat, A. Arques, F. López and M. A. Miranda, Solar photo-catalysis to remove paper mill wastewater pollutants, *Sol. Energy*, 2005, **79**, 393–401.
- X. Fu, Y. Huang, Y. Wang, M. Liang, Y. Yang, Z. Jin, J. Yang, S. Hu and L. Li, Ozonation Catalyzed by Co_xFe₁ Layered Double Hydroxide for the Degradation of P-toluenesulfonic Acid, *Ozone: Sci. Eng.*, 2021, **43**, 163–172.
- W. Xiao, X. Jiang, X. Liu, W. Zhou, Z. N. Garba, I. Lawan, L. Wang and Z. Yuan, Adsorption of organic dyes from wastewater by metal-doped porous carbon materials, *J. Cleaner Prod.*, 2021, **284**, 124773.
- A. A. Özcan and A. Özcan, Investigation of applicability of Electro-Fenton method for the mineralization of naphthol blue black in water, *Chemosphere*, 2018, **202**, 618–625.
- L. Liu, L. Yu, B. Borjigin, Q. Liu, C. Zhao and D. Hou, Fabrication of thin-film composite nanofiltration membranes with improved performance using β -cyclodextrin as monomer for efficient separation of dye/salt mixtures, *Appl. Surf. Sci.*, 2021, **539**, 148284.
- J. Wang and H. Chen, Catalytic ozonation for water and wastewater treatment: Recent advances and perspective, *Sci. Total Environ.*, 2020, **704**, 135249.
- Y. Liu, Y. Zhao and J. Wang, Fenton/Fenton-like processes with in-situ production of hydrogen peroxide/hydroxyl radical for degradation of emerging contaminants: Advances and prospects, *J. Hazard. Mater.*, 2021, **404**, 124191.
- Ç. Çalık and D. İ. Çifçi, Comparison of kinetics and costs of Fenton and photo-Fenton processes used for the treatment of a textile industry wastewater, *J. Environ. Manage.*, 2022, **304**, 114234.
- G. Santana-Martínez, G. Roa-Morales, E. Martín del Campo, R. Romero, B. A. Frontana-Urbe and R. Natividad, Electro-



- Fenton and Electro-Fenton-like with in situ electrogeneration of H_2O_2 and catalyst applied to 4-chlorophenol mineralization, *Electrochim. Acta*, 2016, **195**, 246–256.
- 19 J. Casado, Towards industrial implementation of Electro-Fenton and derived technologies for wastewater treatment: A review, *J. Environ. Chem. Eng.*, 2019, **7**, 102823.
 - 20 T. Yatagai, Y. Ohkawa, D. Kubo and Y. Kawase, Hydroxyl radical generation in electro-Fenton process with a gas-diffusion electrode: Linkages with electro-chemical generation of hydrogen peroxide and iron redox cycle, *J. Environ. Sci. Health, Part A: Toxic/Hazard. Subst. Environ. Eng.*, 2017, **52**, 74–83.
 - 21 W. Zhou, J. Meng, J. Gao and A. N. Alshawabkeh, Hydrogen peroxide generation from O_2 electroreduction for environmental remediation: A state-of-the-art review, *Chemosphere*, 2019, **225**, 588–607.
 - 22 P. Cao, X. Quan, K. Zhao, S. Chen, H. Yu and J. Niu, Selective electrochemical H_2O_2 generation and activation on a bifunctional catalyst for heterogeneous electro-Fenton catalysis, *J. Hazard. Mater.*, 2020, **382**, 121102.
 - 23 X. Liu, Y. Zhou, J. Zhang, L. Luo, Y. Yang, H. Huang, L. Peng, L. Tang and Y. Mu, Insight into electro-Fenton and photo-Fenton for the degradation of antibiotics: Mechanism study and research gaps, *Chem. Eng. J.*, 2018, **347**, 379–397.
 - 24 J. Zheng, Z. Wang, J. Ma, S. Xu and Z. Wu, Development of an electrochemical ceramic membrane filtration system for efficient contaminant removal from waters, *Environ. Sci. Technol.*, 2018, **52**, 4117–4126.
 - 25 B. P. Chaplin, Critical review of electrochemical advanced oxidation processes for water treatment applications, *Env. Sci. Process. Impacts*, 2014, **16**, 1182–1203.
 - 26 L. Ren, J. Ma, M. Chen, Y. Qiao, R. Dai, X. Li and Z. Wang, Recent advances in electrocatalytic membrane for the removal of micropollutants from water and wastewater, *iScience*, 2022, **25**, 104342.
 - 27 D. Kubo and Y. Kawase, Hydroxyl radical generation in electro-Fenton process with in situ electro-chemical production of Fenton reagents by gas-diffusion-electrode cathode and sacrificial iron anode, *J. Clean. Prod.*, 2018, **203**, 685–695.
 - 28 O. García-Rodríguez, J. A. Bañuelos, A. El-Ghenymy, L. A. Godínez, E. Brillas and F. J. Rodríguez-Valadez, Use of a carbon felt-iron oxide air-diffusion cathode for the mineralization of Malachite Green dye by heterogeneous electro-Fenton and UVA photoelectro-Fenton processes, *J. Electroanal. Chem.*, 2016, **767**, 40–48.
 - 29 C. A. Martínez-Huitle, M. A. Rodrigo, I. Sirés and O. Scialdone, Single and Coupled Electrochemical Processes and Reactors for the Abatement of Organic Water Pollutants: A Critical Review, *Chem. Rev.*, 2015, **115**, 13362–13407.
 - 30 E. Brillas, I. Sirés and M. A. Oturan, Electro-Fenton Process and Related Electrochemical Technologies Based on Fenton's Reaction Chemistry, *Chem. Rev.*, 2009, **109**, 6570–6631.
 - 31 G. Pliego, J. A. Zazo, P. García-Muñoz, M. Muñoz, J. A. Casas and J. J. Rodríguez, Trends in the Intensification of the Fenton Process for Wastewater Treatment: An Overview, *Crit. Rev. Environ. Sci. Technol.*, 2015, **45**, 2611–2692.
 - 32 J. Zheng, S. Xu, Z. Wu and Z. Wang, Removal of p-chloroaniline from polluted waters using a cathodic electrochemical ceramic membrane reactor, *Sep. Purif. Technol.*, 2019, **211**, 753–763.
 - 33 İ. Y. Köktaş and Ö. Gökkuş, Removal of salicylic acid by electrochemical processes using stainless steel and platinum anodes, *Chemosphere*, 2022, **293**, 133566.
 - 34 L. Wang, M. Cao, Z. Ai and L. Zhang, Design of a Highly Efficient and Wide pH Electro-Fenton Oxidation System with Molecular Oxygen Activated by Ferrous-Tetrapolyphosphate Complex, *Environ. Sci. Technol.*, 2015, **49**, 3032–3039.
 - 35 N. Barhoumi, N. Oturan, S. Ammar, A. Gadri, M. A. Oturan and E. Brillas, Enhanced degradation of the antibiotic tetracycline by heterogeneous electro-Fenton with pyrite catalysis, *Environ. Chem. Lett.*, 2017, **15**, 689–693.
 - 36 J. Anotai, C.-C. Su, Y.-C. Tsai and M.-C. Lu, Effect of hydrogen peroxide on aniline oxidation by electro-Fenton and fluidized-bed Fenton processes, *J. Hazard. Mater.*, 2010, **183**, 888–893.
 - 37 T. X. Huong Le, L. F. Dumée, S. Lacour, M. Rivallin, Z. Yi, L. Kong, M. Bechelany and M. Cretin, Hybrid graphene-decorated metal hollow fibre membrane reactors for efficient electro-Fenton - Filtration co-processes, *J. Membr. Sci.*, 2019, **587**, 117182.
 - 38 Y.-P. Chen, L.-M. Yang, J. Paul Chen and Y.-M. Zheng, Electrospun spongy zero-valent iron as excellent electro-Fenton catalyst for enhanced sulfathiazole removal by a combination of adsorption and electro-catalytic oxidation, *J. Hazard. Mater.*, 2019, **371**, 576–585.
 - 39 Ö. Gökkuş, Oxidative degradation of Basic Black 3 by electro-generated Fenton's reagent using carbon fiber cathode, *Clean Technol. Environ. Policy*, 2016, **18**, 1525–1534.
 - 40 Y. Jing and B. P. Chaplin, Mechanistic study of the validity of using hydroxyl radical probes to characterize electrochemical advanced oxidation processes, *Environ. Sci. Technol.*, 2017, **51**, 2355–2365.
 - 41 M. Chen, L. Ren, K. Qi, Q. Li, M. Lai, Y. Li, X. Li and Z. Wang, Enhanced removal of pharmaceuticals and personal care products from real municipal wastewater using an electrochemical membrane bioreactor, *Bioresour. Technol.*, 2020, **311**, 123579.
 - 42 Y. Bai, T. Sun, L. T. Angenent, S. B. Haderlein and A. Kappler, Electron Hopping Enables Rapid Electron Transfer between Quinone-/Hydroquinone-Containing Organic Molecules in Microbial Iron(III) Mineral Reduction, *Environ. Sci. Technol.*, 2020, **54**, 10646–10653.
 - 43 P. Hongsawat and A. S. Vangnai, Biodegradation pathways of chloroanilines by *Acinetobacter baylyi* strain GFJ2, *J. Hazard. Mater.*, 2011, **186**, 1300–1307.
 - 44 P. Y. Lee and C. Y. Chen, Toxicity and quantitative structure-activity relationships of benzoic acids to *Pseudokirchneriella subcapitata*, *J. Hazard. Mater.*, 2009, **165**, 156–161.

